Type of the Paper (Article)

Analysis of the thermo-mechanical behaviour of the EU DEMO Water-Cooled Lithium Lead Central Outboard Blanket Segment under an optimized thermal field.

Ilenia Catanzaro [1]*, Gaetano Bongiovì [1] and Pietro Alessandro Di Maio [1]

[1] Department of Engineering, University of Palermo, Viale delle Scienze, Ed. 6, 90128 Palermo, Italy
* Correspondence: ilenia.catanzaro@unipa.it

Abstract: Within the framework of the EUROfusion research activities on the DEMO Water-Cooled Lithium Lead (WCLL) Breeding Blanket (BB) design, a research campaign has been performed to preliminarily optimize, from the thermal point of view, the WCLL Central Outboard Blanket (COB) segment in order to investigate its structural behaviour under a realistic thermal field. In paticular, a campaign of thermal analyses has been performed to optimize the Double Walled Tubes and Segment Box cooling channels geometric configurations along the poloidal extension of the WCLL COB segment, in order to obtain a temperature spatial distribution fulfilling the thermal design requirement. Then, the thermomechanical analysis of the WCLL COB segment under Normal Operation (NO, representing nominal conditions), Upper Vertical Displacements Event (UVDE, representing a plasma disruption event) and Over-Pressurization (OP, representing an in-box loss of coolant accident) scenarios have been carried out, assuming the previously obtained thermal field, to realistically predict displacement and stress fields. Finally, a stress linearization procedure has allowed comparing the stress values obtained in some critical regions of the structure with the criteria prescribed by the reference design standard RCC-MRx. A theoretical-numerical approach based on the Finite Element Method (FEM) has been followed using the commercial code Abaqus v. 6.14.

Keywords: DEMO WCLL; Breeding Blanket; thermo-mechanics; FEM analysis.

1. Introduction

Within the framework of the conceptual design of the EU-DEMO Breeding Blanket (BB) [1,2], the University of Palermo is involved in the design of the Water-Cooled Lithium Lead (WCLL) BB foreseen for the European DEMO fusion reactor. One of the main objectives of the research activity is the development of a geometric layout for the WCLL Central Outboard Blanket (COB) segment robust enough to fulfil all the prescribed design requirements. To this purpose, the assessment of its thermo-mechanical behaviour under different loading conditions plays a key role and, in this regard, the availability of a realistic and detailed thermal field for the whole WCLL COB segment is pivotal. Nevertheless, the WCLL COB design presented at the end of the pre-conceptual phase [3] was not mature enough to allow reliable thermal-hydraulic assessments for the prediction of its thermal field. In any case, such a kind of analysis would require a huge modelling effort, followed by a tremendous computational burden, which would imply the adoption of strong assumptions leading to a certain margin of uncertainties in the results [4]. Hence, an alternative procedure has been developed [5] and applied in this work in order to predict a reliable 3D thermal field for the WCLL COB without performing its full thermal-hydraulic analysis, taking into account the radial and poloidal dependence of the thermal loads (namely nuclear heating and heat flux on the FW surface).

Afterwards, once predicted the 3D thermal field of the WCLL COB segment, its structural behaviour has been evaluated under different steady-state loading scenarios. First, the Normal Operation (NO) scenario, representing the normal operating conditions and thus falling under service Level A of the RCC-MRx [6] structural design code, has been taken into account. Secondly, proper accidental loading scenarios have been set-up, derived from two off-normal reference events: the Upper Vertical Displacements Event (UVDE) and the in-box Loss of Coolant Accident (LOCA). The UVDE is an off-normal event reproducing a plasma disruption due to an uncontrolled vertical motion of the plasma volume, classified as Level C. Instead, the in-box LOCA is the design driving accident for the BB and therefore it is classified as Level D in the RCC-MRx design code. Its associated loading conditions form the Over-pressurization (OP) steady state loading scenario. The thermo-mechanical behaviour of the whole WCLL COB segment has been therefore assessed in terms of displacement and equivalent Von Mises stress fields. Moreover, a stress linearization procedure has been performed within some critical regions, in order to evaluate the stress level by means of the design rules prescribed by the French nuclear code RCC-MRx, currently the reference one for the DEMO reactor, performing a stress linearization procedure along some paths within the structure.

A theoretical-numerical approach based on the Finite Element Method (FEM) has been followed. The commercial code Abaqus v. 6.14 [7], considered as one of the reference FEM codes by the international scientific community involved in the nuclear fusion research, has been utilized. The obtained results are herewith presented and critically discussed. To this goal, the adopted methodology and the structure of the paper are reported in the following section 2.

2. The adopted methodology

As stated in the previous section, the WCLL COB design passed through the DEMO pre-conceptual gate review was not detailed enough to allow reliable thermal-hydraulic analysis for the detailed calculation of its thermal field. At the same time, the availability of a reliable and detailed 3D temperature spatial distribution for the whole segment is crucial for the assessment of its thermomechanical performances in different loading scenarios. Hence, in this work, an alternative procedure has been applied to get a reliable estimation of the thermal field arising within the WCLL COB segment without performing its whole thermal-hydraulic assessment.

To this purpose it has to be observed that each BB segment could be ideally subdivided into 7 poloidal regions [3,8], each characterized by a certain set of distributed thermal loads (namely plasma heat flux, nuclear heating and decay heat power density) representative of the operating conditions of the considered region (Figure 1). In this work, the equatorial radial-toroidal elementary cell of each of the 7 COB poloidal regions (as depicted, as an example, for O5 region in Figure 1) has been assessed from the thermal point of view (section 3.1), taking into account the 3D nature of the pertinent thermal loads and the reference geometric layout, described in the following. To this purpose, considering the suggested Eurofer maximum temperature limit equal to 550 °C within the structural components [3], it has been found that a thermal optimization of the WCLL COB segment's cooling layout (namely first wall channels and breeding zone cooling tubes) was necessary in order to obtain, for each of the 7 equatorial cells assessed, a thermal field fulfilling the above said requirement minimizing the number of tubes.

Hence, alternative geometric layouts have been conceived and assessed assuming, for each of the 7 poloidal regions, the corresponding set of thermal loads (section 3.2). Once obtained, for each of the 7 equatorial cells assessed, an optimized geometric layout for the cooling system and the pertinent thermal field fulfilling the design requirement, an interpolation procedure has been performed in order to carry out 7 different sets of interpolating functions of the radial and toroidal variable capable of reproducing the calculated thermal fields with a high level of confidence. Then, the found sets of interpolating functions have been applied to the 7 poloidal regions (namely to the whole O1,

O2, …, O7 region) so to reproduce, on the whole COB segment, a detailed 3D thermal field originated by the radial-poloidal dependent thermal loads and fulfilling the prescribed design thermal requirement.

At this point, the structural assessment (section 4) of the whole WCLL COB under the obtained optimized 3D thermal field has been performed, under the nominal and accidental steady state loading scenarios described in the following. The obtained results have been used to assess the displacement and Von mises equivalent stress fields and to perform a stress linearization procedure in some critical areas, so to verify the fulfilment of the structural design criteria, namely the criteria prescribed by the RCC-MRx structural design code.

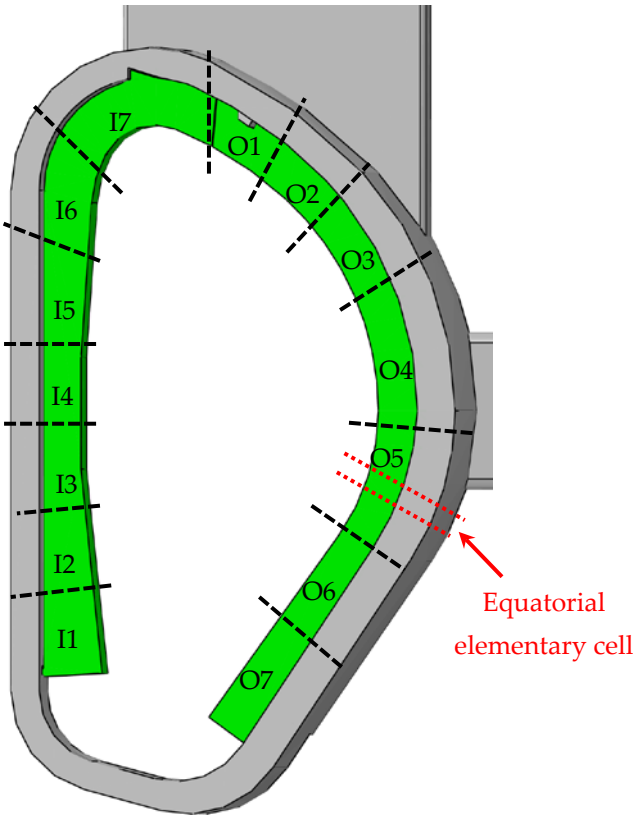

Figure 1. Poloidal Segmentation of the DEMO BB and numbering of the Inboard and Outboard poloidal regions.

3. Thermal Analysis of the WCLL COB segment

In order to assess the thermo-mechanical performances of the WCLL COB segment, the first step has been the determination of a thermal field for the whole segment. To this purpose, the necessity to fulfil the thermal design requirement on the maximum Eurofer temperature [3] has led to optimize the WCLL COB segment's cooling scheme. In this framework, the first step has been the thermal analysis of the reference layout of the equatorial radial-toroidal elementary cell of each of the 7 COB poloidal regions (from O1 to O7, Figure 1). Afterwards, the thermal optimization of those regions not-fulfilling the prescribed requirement has been performed with the aim of obtaining a thermal field characterized by the maximum Eurofer temperature within structural components lower than 550 °C [3].

3.1. Thermal analysis of the equatorial radial-toroidal cell of each of the 7 COB poloidal regions

The thermal analysis of the reference layout of the equatorial radial-toroidal elementary cell of each of the 7 COB poloidal regions has been performed under the steady state normal operation loading conditions foreseen for the WCLL COB.

3.1.1. The reference geometric layout

According with the Single Module Segmentation (SMS) concept, the WCLL COB Segment is composed by a single elementary cell, identified by two horizontal Stiffening Plates (SPs), that repeats along the poloidal direction from a Cap to another, which vertically close the segment. The structure, depicted in Figure 2, is mainly characterized by the Segment Box (SB), divisible into First Wall (FW), with the 2mm-thick of W-armour (coloured in orange in Figure 2), and the Side Walls (SWs) that laterally close the SB. Moreover, the structure is closed in the back by the complex of Back Plate (BP), water and breeder manifolds and the Back Supporting Structure (BSS), connected to the attachment system (coloured in grey in Figure 2), aimed to mechanically connect the Segment to the Vacuum Vessel (VV). The breeder flows inside the box, in the region called Breeder Zone (BZ) [3], which is reinforced by means of the SPs. In particular, the SPs grid is composed by horizontal (or toroidal-radial) and vertical (or poloidal-radial) SPs, respectively with a thickness equal to 10 and 12 mm. A bundle of 22 cooling tubes per cell (Figure 3), Double Walled Tubes (DWTs), immersed in the PbLi, has the role of cooling the BZ, instead, the FW-SW-FW region is cooled by means of 7x7 m^2 cooling channels located into the SB.

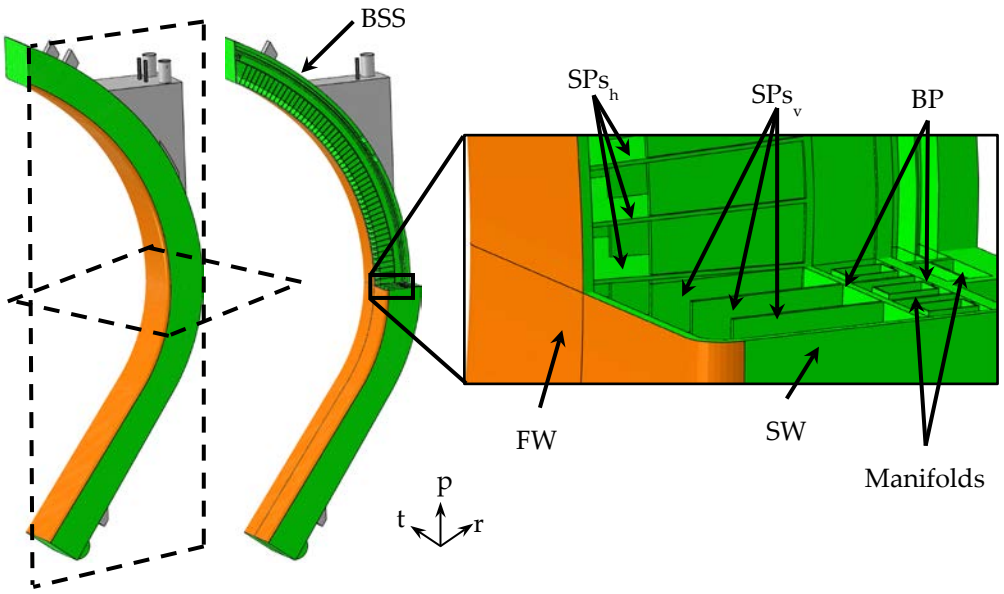

Figure 2. COB Segment architecture and detail of the main components.

In order to observe the different thermal loads characterizing the poloidal extension of the segment, the number of cooling channels per cell varies along the COB segment [3], following the aforementioned poloidal segmentation. In particular, 4 channels per cell are foreseen for each poloidal region with exception of O7 region in which 6 channels are foreseen. Instead, only one DWTs configuration has been preliminary selected for all the elementary cells along the segment. In particular, the chosen DWTs layout, named v06b as reported in [3] , consisting of 22 C-shaped double-walled tubes, with hydraulic diameter of 8 mm and an external diameter equal to 13.5 mm, each with different position and radius. In Figure 3 the DWTs layout in an elementary cell (namely an equatorial radial-toroidal cell) and the water path inside them (in which red arrows indicate the inlet and green the outlet), with the BZ recirculation scheme (highlighted in orange), is reported.

In the present work, two realistic 3D geometric models of a couple of elementary cells (Figure 4), equipped with 4 and 6 cooling channels respectively and the WCLL v06b DWTs layout, representing a portion of the whole COB segment, have been set up in order to realistically simulate its thermal behaviour. Given that the reference DWTs layout is the same along the whole segment, the geometric model envisaging 4 FW

channels represents the equatorial radial-toroidal cell of regions from O1 to O6, whereas the model with a FW equipped with 6 cooling channels represent the equatorial elementary cell of the O7 poloidal region.

Two detailed FEM models have been set-up, each one composed of ~13M nodes connected in ~5M linear hexahedral and tetrahedral elements, including the Eurofer structure, tungsten layer, DWTs, breeder and water coolant flowing inside FW channels and DWTs.

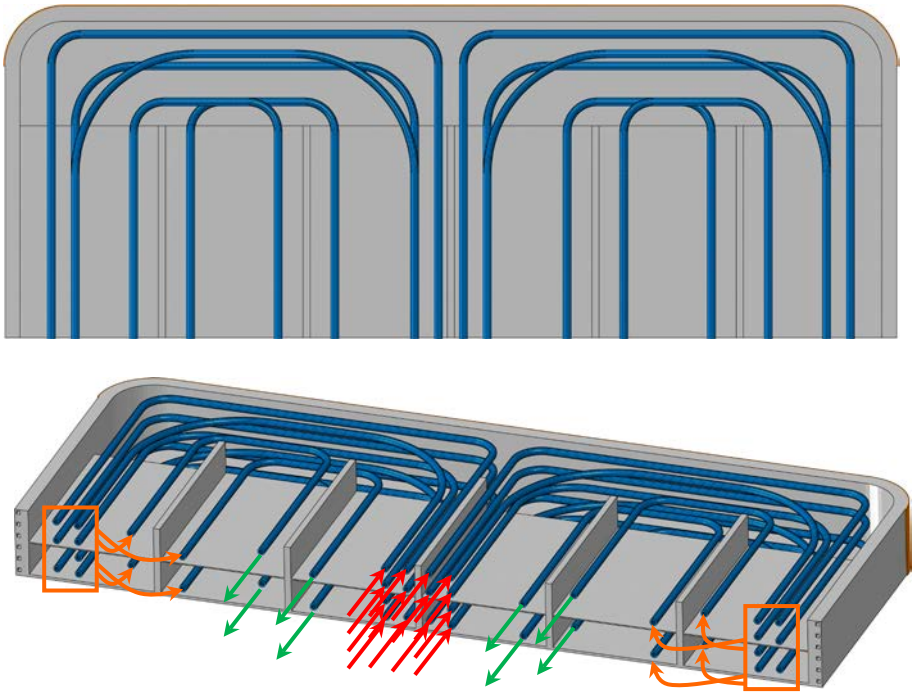

Figure 3. WCLL v06b DWTs layout and recirculation scheme (inlet in red, first outlet/recirculation in orange, exit in green).

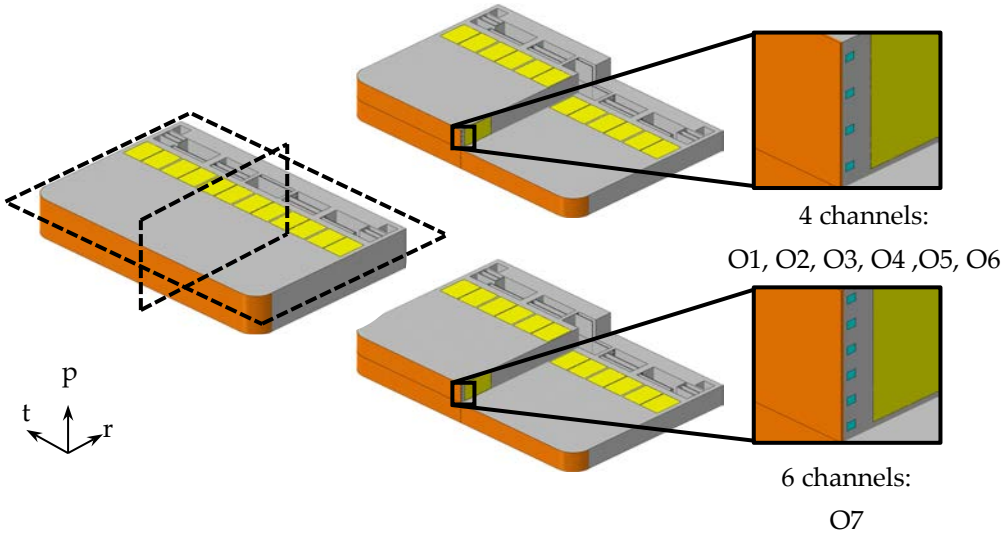

Figure 4. Models of the two elementary cells equipped with 4 and 6 cooling channels.

3.1.2. Loads and Boundary Conditions

In order to perform the thermal analysis, a set of loads and boundary conditions, pertinent to the Normal Operation steady state loading scenario, has been considered for each model taken into account.

The temperature-dependent properties of materials have been taken into account. In particular, for Eurofer, Pb-15.7Li and Tungsten, the physical properties have been drawn from [9,10,11].

A non-uniform value of heat flux (Φ), due to particles and radiation arising from plasma, for each COB poloidal regions has been imposed onto the straight and bend FW plasma facing surface. The selected heat flux values [12], assumed at the end of flat-top, are reported in Table 1. In particular, the values reported in Table 1 have been applied onto the straight FW surface. Instead, for the bend FW surfaces a decreasing value according to a cosine-dependent law has been assumed considering the values reported in Table 1 as maximum ones:

$$\Phi_{FWbend} = \Phi_{FW} \cdot \cos\alpha \quad (1)$$

where Φ_{FWbend} is the value imposed to the bend FW surface, Φ_{FW} the values reported in Table 1 as maximum ones and α varies between 0, corresponding to the start of the bend region, and $\pi/2$, to the SW.

Moreover, a spatial distribution of volumetric density of nuclear-deposited heat power, derived from neutron transport analysis [3], has been imposed to each FEM model to simulate the distributed power deposition as a result of the neutrons, gamma photons and nuclei interactions. Moreover, differently from the previous thermal analysis carried out, also the contribution of the decay heat, caused by the activated materials, has been taken into account [13]. In particular, the decay heat power spatial distribution calculated at the shut-down has been assumed for the normal operation scenario, as it contributes to heat the structure.

Since, at present, the spatial distributions of nuclear power and decay heat are calculated only for the O4 region, the analogous spatial distributions for the other 6 poloidal regions have been obtained using the ratio between the Neutron Wall Loadings (NWLs) in the i-th region and that in the O4 region as scaling factor. The adopted NWLs average values for each COB region [3] are reported in Table 1.

Table 1. Total Heat Flux and average NWL poloidal distribution.

	O1	**O2**	**O3**	**O4**	**O5**	**O6**	**O7**
Maximum Heat Flux [MW/m²]	0.24	0.27	0.26	0.27	0.27	0.67	0.67
Average NWL [MW/m²]	0.9834	1.1592	1.2802	1.3335	1.3287	1.1844	0.7539

Moreover, in order to simulate the thermal contact of the PbLi with the SB and DWTs breeder-wetted surfaces, a pure diffusive heat transfer contact with a conservative value of thermal conductance equal to 100 [kW/m²·°C] has been assumed. The breeder, since it flows very slowly, due to the action of buoyancy and magneto-hydrodynamics forces, in fact, can be considered as stagnant. Then, the DWTs and the SB structure are considered as a continuum concerning the thermomechanical behaviour.

Finally, a forced convective heat transfer between coolant and water-wetted surfaces adopting a proper thermal contact has been considered. In particular, a counter-current flow path has been imposed for the FW-SW cooling water, instead, concerning the DWTs cooling water, the path shown in Figure 3 has been simulated and the recirculation system has been properly modelled. To reproduce the DWTs water path, the tubes have been divided into two groups, the first, in which the water enters at 295 °C, including 14 tubes and the second, where the recirculation takes place, includes 8 tubes. In order to correctly simulate the recirculation system, the average water outlet temperature, namely mixing temperature, of the first group has been calculated and set as the water inlet temperature of the second group of tubes, by means of a proper Abaqus procedure.

A first attempt value of mass flow rate has been selected for each group of DWTs

and channel, and a related heat transfer coefficient, calculated using the Dittus & Boelter (D&B) correlation [14], has been considered. In particular, an inlet temperature of 295 °C and a water temperature difference (ΔT) between inlet and outlet equal to 33 °C have been imposed for the calculation. So, the heat transfer coefficients (HTCs) and the mass flow rates values needed to ensure the selected ΔT have been calculated by means of an iterative procedure [15]. Lastly, adopting a "frozen field" calculation approach, it has been possible calculating the water bulk temperature along each channel/tube abscissa. In particular, the adopted iterative procedure consists of imposing the bulk temperature and mass flow rate (i.e. mass flow per unit area) at the inlet of each cooling tubes or channels together with the "first attempt" (i.e. calculated using the D&B correlation) HTC. The latter does not change during the current iteration. Hence, such kind of approach allows calculating the bulk temperature along the flow direction and using it for the imposition of the convective heat transfer condition. The thermal analysis has been iterated so to obtain an HTC value able to produce a thermal rise between water inlet and outlet of ~33 °C. In Table 2 the HTC values adopted for each poloidal region in the last iteration for the complex of cooling channels and DWTs, where HTC_{CC}, HTC_{DWTs} and $HTC_{DWTs,rec}$ indicate the HTC values used for the cooling channels, first group of DWTs and recirculation DWTs respectively, are reported.

Table 2. HTC values used for cooling channels and DWTs coolant.

	O1	O2	O3	O4	O5	O6	O7
HTC_{CC} [W/m²·K]	31368	33609	34490	35570	35518	38895	36167
HTC_{DWTs} [W/m²·K]	16965	19901	19258	19905	19847	20033	13576
$HTC_{DWTs,rec}$ [W/m²·K]	26545	31139	33530	34656	34556	31346	21243

3.1.3. Results

A steady-state thermal analysis has been performed for the equatorial cells of each of the 7 COB poloidal regions with the aim of investigating their thermal behaviour under the loads and boundary conditions they undergo. For the sake of brevity, the maximum temperature predicted in each region is reported in Table 3, where the temperatures exceeding the suggested limit value of 550 °C are reported in red. Looking at the temperature values reached on SPs and FW, as the baffle plates do not play a structural role, only O1 and O7 regions do not overtake the Eurofer structural material limit temperature, set to 550 °C, whereas all the others exceed this value. Hence, for the latter regions, an optimization of the DWTs layout is necessary. Moreover, looking at the results reported in Table 3, the O6 region shows a temperature higher than the temperature limit on the FW too. This result suggests that this poloidal region must be equipped with 6 channels, as in O7. Hence, as to O6 region, a further optimization of the FW channels is necessary.

As an example, the thermal field obtained within the structural material of the O4 region, corresponding to the equatorial region of the whole COB segment, is depicted in Figure 5 whereas in Figure 6 the temperature spatial distribution within Eurofer of the O6 equatorial cells is depicted.

Table 3. Maximum temperature per region equipped with v06b layout.

	O1	O2	O3	O4	O5	O6	O7
Tmax on FW [°C]	478.2	503.3	519.0	526.6	525.9	566.4	479.2
Tmax on SPs [°C]	546.7	580.5	603.1	612.9	612.1	585.2	501.0

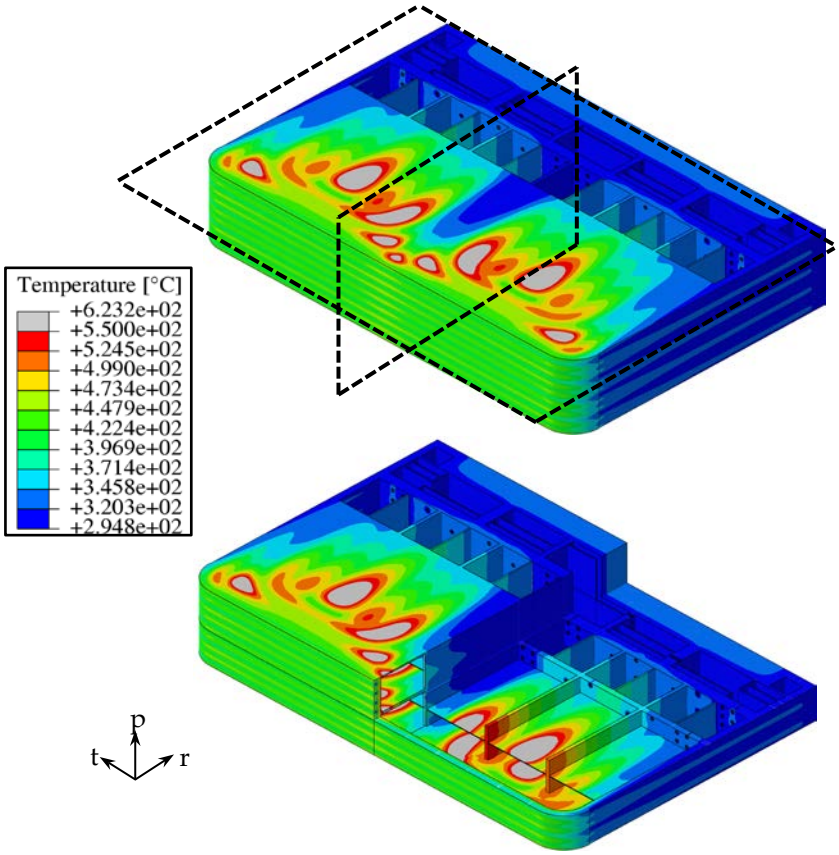

Figure 5. Thermal field raised within the Eurofer domain of the O4 region.

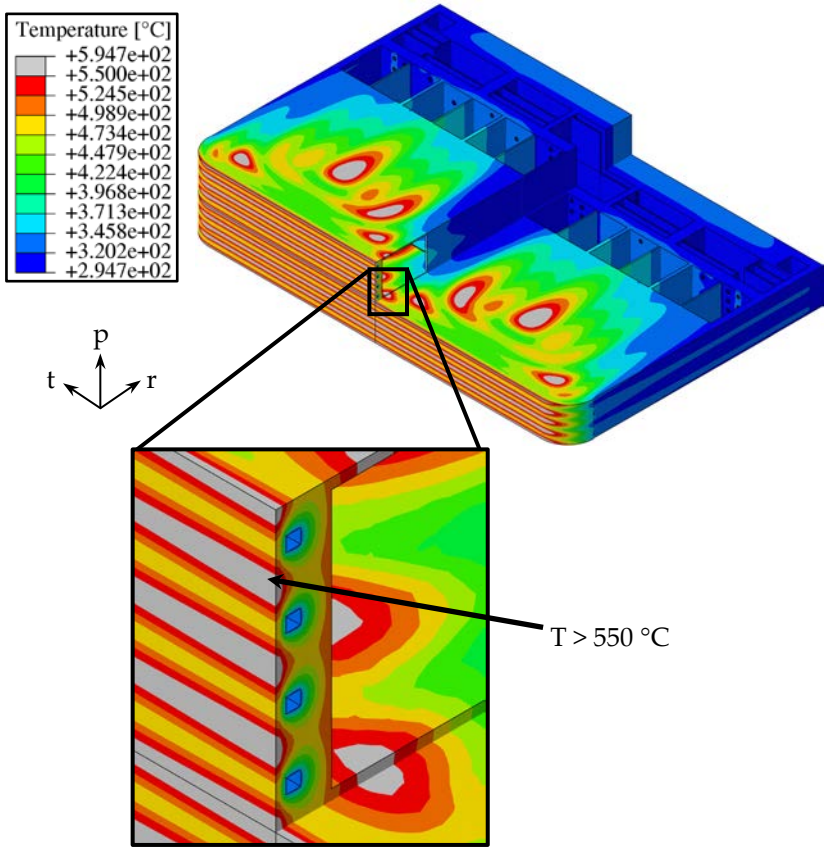

Figure 6. Thermal field raised within the Eurofer domain of the O6 region.

3.2. WCLL COB thermal optimization and determination of its thermal field

The results obtained from the thermal analysis of the reference geometric layout of the equatorial elementary cell of each WCLL COB poloidal region allow concluding that, as to O2, O3, O4 and O5 region, a thermal optimization of the DWTs layout is necessary to allow fulfilling the requirement on the maximum Eurofer temperature. In addition, for O6 region, also the FW channels should be optimized since critical temperature values are predicted within both FW and SPs. Lastly, once obtained the optimized thermal field for each of the 7 poloidal regions, a thermal field for the whole WCLL COB segment can be derived.

3.2.1. DWTs and FW channels thermal optimization

In order to thermally optimize the WCLL COB segment, three alternative DWTs layouts foreseeing 22, 24 and 26 "crossed" DWTs per elementary cell have been set-up, foreseeing the crossing of the first row of tubes to remove the temperature hotspot in the central region of the cell (Fig. 6). Moreover, the configurations with 24 and 26 DWTs per slice have been obtained moving along the radial and the toroidal directions the first two rows of tubes and adding a new row of tubes, consisting of 2 or 4 tubes respectively (Figure 7 and 8). Regarding O6 region, the FW-SW has been equipped with 6 channels per cell as well.

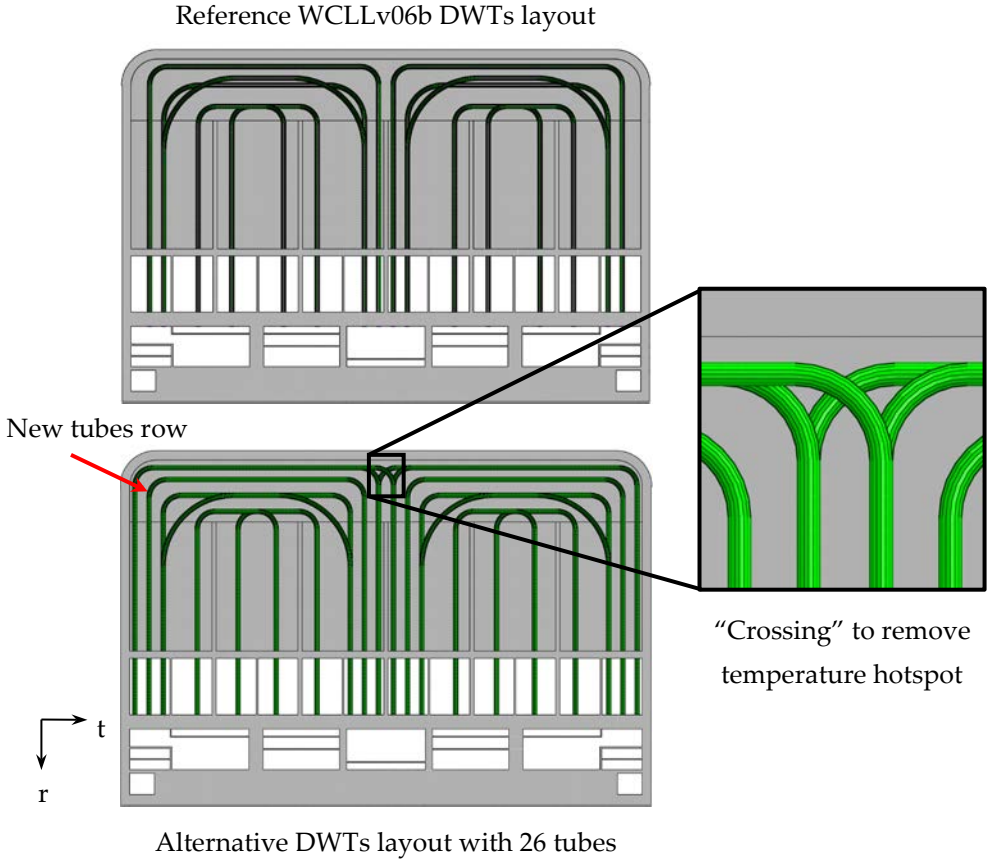

Figure 7. Alternative DWTs layout and detail of the crossing tubes.

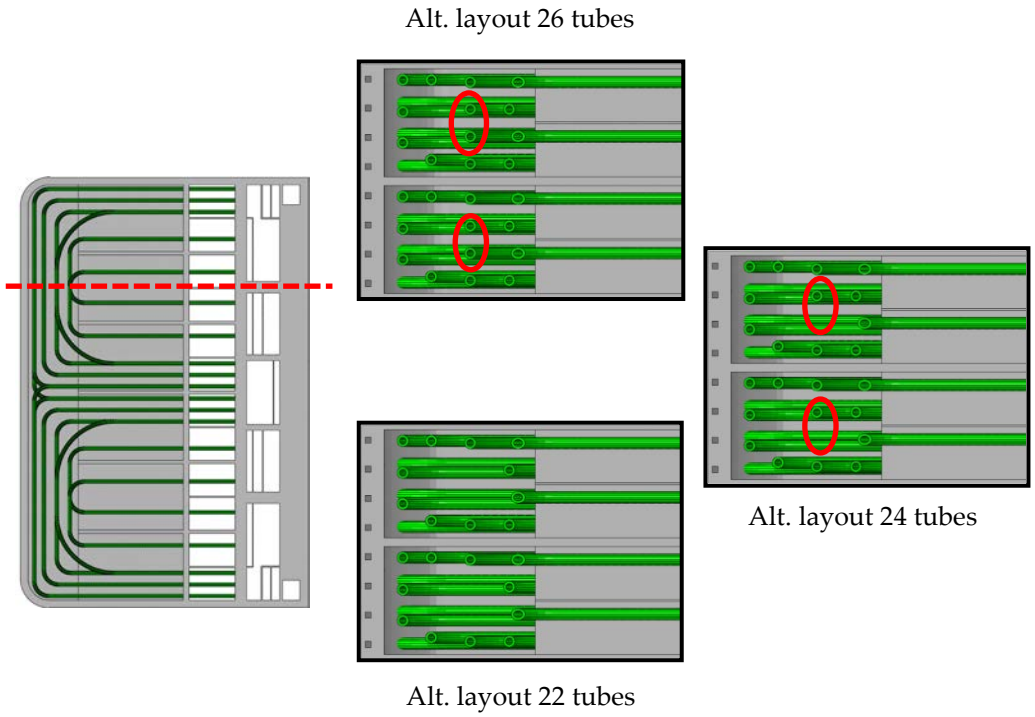

Figure 8. Alternative DWTs layout equipped with 26, 24, and 22 tubes.

In order to study the thermal behaviour of the three alternative DWTs configurations on each WCLL COB poloidal region to be optimized, a couple of elementary cells equipped with 26, 24 and 22 "crossed" DWTs have been studied. Three FEM models, with a mesh composed of ~3M nodes connected in ~4M linear hexahedral and tetrahedral elements, have been set-up for each region. Then, loads and boundary conditions already discussed above have been considered. Finally, a parametric set of thermal analysis has been launched with the aim of achieving the DWTs configuration for each COB poloidal region capable of removing the heat, while keeping the temperature below 550 °C, with the minimum number of tubes.

Results are synthetically summarized in Table 4, where the DWTs layout configuration selected, the number of FW-SW channels for each COB region and, moreover, the corresponding maximum temperature reached on the SPs and FW is shown. In particular, in Table 4 the labels "v06b ref.", "alt. 22" and "alt. 24" indicate the reference layout v06b and the two alternative DWTs configurations equipped with 22 and 24 tubes, respectively.

Table 4. BZ and FW-SW cooling layout per poloidal region.

	O1	O2	O3	O4	O5	O6	O7
n. channels	4	4	4	4	4	6	6
DWTs layout	v06b ref.	alt. 22	alt. 24	alt. 24	alt. 24	alt.22	v06b ref.
Tmax on SPs [°C]	546.7	534.0	531.4	538.9	538.2	539.2	501.0
Tmax of FW [°C]	478.2	484.6	497.8	504.6	504.0	474.6	479.2

3.2.2. Determination of a thermal field for the whole WCLL COB segment

The outcomes of the previous optimization campaign have been used in order to represent in the most realistic way the thermal field arising in the whole WCLL COB segment. Indeed, starting from the optimized thermal field calculated in each of the 7 equatorial cells, an interpolation procedure [5] has been performed to obtain 7 different set of functions of the radial and the toroidal variable. Then, a proper Fortran subroutine (named "UDISP") has been set-up to provide the poloidal dependence so to obtain a different 3D thermal field for each of the 7 WCLL COB poloidal regions. Lastly, the 7 thermal fields have been stitched together to give the 3D temperature spatial distribution for the whole WCLL COB segment.

To perform the interpolation, each equatorial cell has been divided into 13 different regions: one for the SW-FW-SW and one for the manifolds region, one for each vertical SP, for a total of 5 regions, and 6 for each horizontal SP, identified by the 5 poloidal-radial SPs. Successively, a polynomial function of the radial and toroidal variables has been drawn for each region to represent its temperature distributions. A set of 13 polynomial functions has been then build up for each COB poloidal region to reproduce the thermal field in the most accurate way. In particular, a 14^{th} degree polynomial function of two variables (r and t directions) has been selected for the SW-FW-SW regions, up to 9^{th} degree polynomial function of one variable (r direction) for the manifolds, up to 10^{th} degree polynomial functions of two variables (r and t directions) for each SPh and up to 14^{th} degree polynomial functions of one variable (r direction) for each SPv. Concerning the Caps, since their cooling system has not yet been studied in detail, a polynomial function of one variable (r direction) has been obtained from the SWs region and applied to the whole plate, while, on the corresponding FW region, the same polynomial function of the nearest poloidal region (namely O1 and O7) has been used.

The obtained thermal field is depicted in Figure 9 with some details at different poloidal heights of the segment. Moreover, a uniform temperature value of 300°C has been considered for the supports (namely the attachment system) in charge of connecting the segment to the VV.

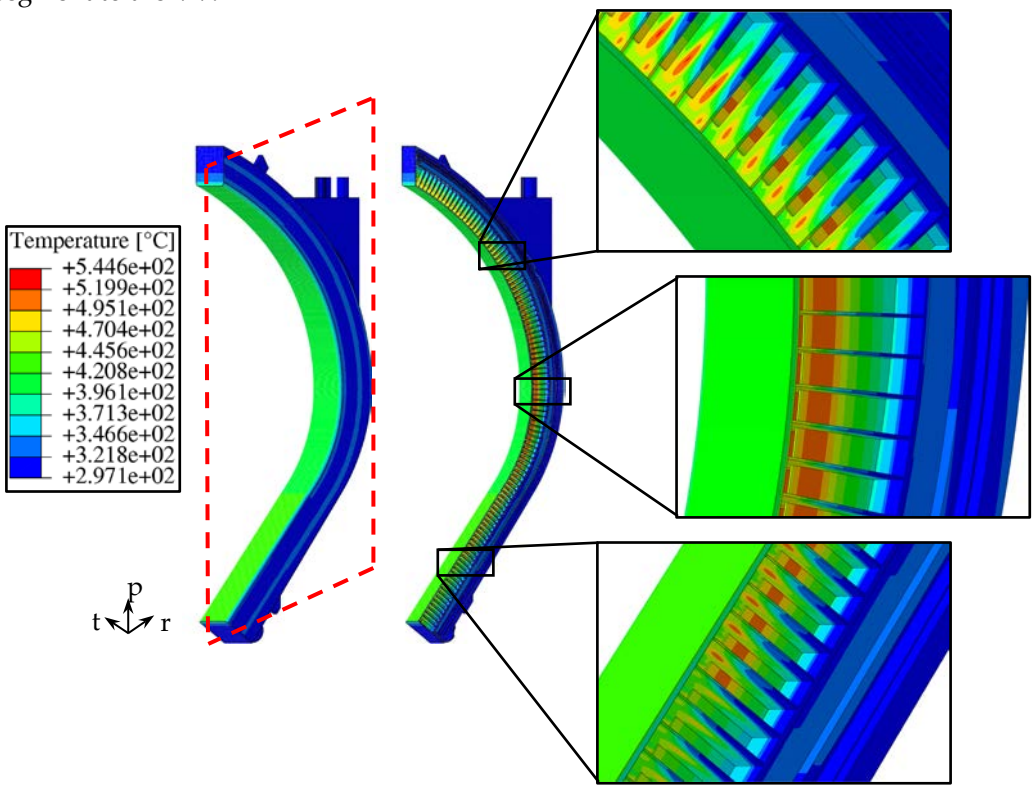

Figure 9 Thermal field obtained for the whole WCLL COB segment by the interpolation procedure.

4. Structural Analysis of the reference COB segment

Once obtained a reliable and detailed thermal field of the whole WCLL COB segment, its structural performances under different steady state loading scenarios have been assessed. To this end, since Baffle Plates and DWTs have no structural role, they are not been considered in the pertinent FEM model, in order to reduce the computational burden. Therefore, a FEM model has been created on Abaqus and a mesh composed of ~3.2M nodes connected in ~8.7M tetrahedral and hexahedral elements has been set up.

4.1. Loads and Boundary conditions

The assessment of the thermo-mechanical behaviour of the reference COB segment foresees its evaluation under different steady state loading scenario. In particular, the loading scenarios considered are: the Normal Operation (NO), the Over-Pressurization (OP) and the Upper Vertical Displacement Event (UVDE). The NO scenario represents the nominal conditions that the WCLL COB is supposed to undergo during flat-top plasma. Instead, the OP scenario is a load combination derived from the in-box LOCA. This scenario is derived supposing that the occurrence of an in-box LOCA suddenly pressurizes the whole SB. Lastly, the UVDE scenario takes into account the very intense electro-magnetic loads due to an uncontrolled vertical movement of the plasma causing a plasma disruption. The loading conditions relevant to the steady state scenario of NO, OP and UVDE are classified as Level A, Level D and Level C, respectively, in the RCC-MRx structural design code.

In order to predict the structural response of the COB segment, a set of loads and boundary conditions has been assumed to reproduce the three assessed loading scenarios [16].

- internal pressure distribution according to the considered loading scenario;
- mechanical restraints;
- gravity load;
- non-uniform deformation thermal field;
- electro-magnetic loads.

Since neither breeder nor water have been modelled, in order to reproduce their mechanical effect, a uniform pressure value has been imposed to all the wetted surfaces. In particular, the design pressure value, calculated as the nominal one times a safety factor equal to 1.15 [16], has been imposed onto both breeder-wetted and water-wetted surfaces. So, for NO and UVDE loading scenario, a pressure equal to 17.825 MPa has been considered for all the water-wetted surfaces, instead a value equal to 0.575 has been applied to the surfaces wetted by the PbLi. Instead, an equal value of 17.825 has been considered for all the internal wetted surfaces in the OP loading scenario.

Additionally, the reference attachment system consists in a set of supports aimed at fixing the blanket segments to the VV and, at the same time, withstanding very large electro-magnetic loads, thermal deformations and maintaining a good alignment of the FW. The supports are located at the bottom and at the top part of the segment and each face of these supports works along a particular direction, as reported in Figure 10, thus ensuring the segment connection with the VV [17]. These contacts are simulated by means of springs, particular Abaqus element, in correspondence of each surface. So, each of the springs is assigned a specific value of elastic constant.

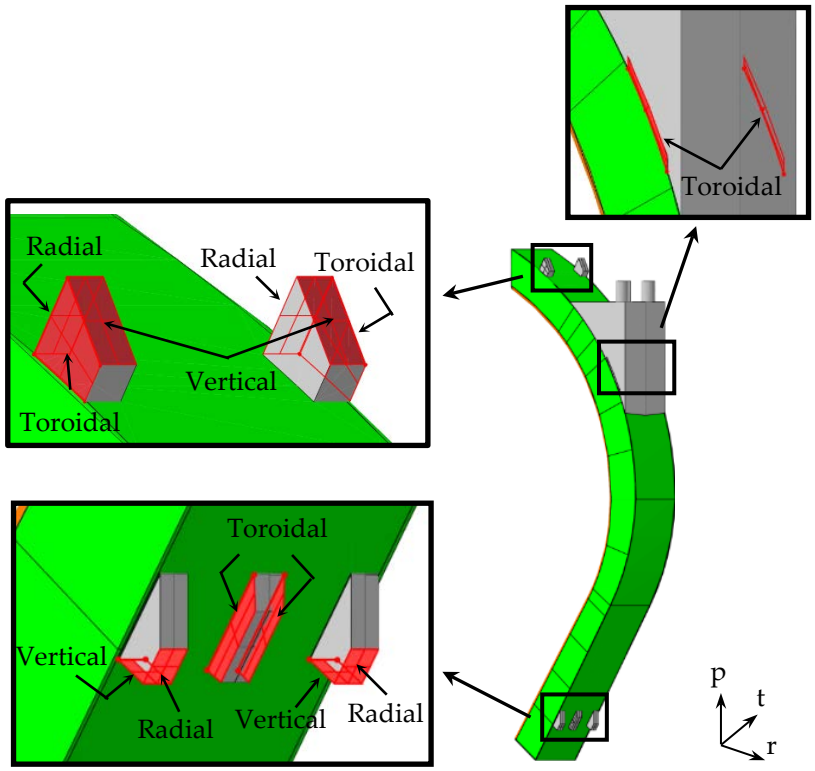

Figure 10. WCLL COB attachment system and indication of the directions of action of the springs.

The gravitational load has been also applied onto the whole model. However, since liquid metal breeder and coolant have not been modelled, their contribution has been taken into account using an Eurofer equivalent density, as already done in previous analyses. The equivalent density value has been obtained assuming that the percentage of steel, water and breeder are equal to that calculated for the equatorial region. So, temperature-dependent properties of Tungsten and Eurofer structural steel [9,11] have been taken into account and implemented in the model, properly modify the Eurofer density values.

As to the non-uniform deformation thermal field, it arises within the structure as effect of the imposed temperature spatial distribution (Figure 9) and the volumetric expansion coefficient.

Finally, the electro-magnetic loads have also been considered for all the assessed steady state loading scenarios. In fact, their action during normal and off-normal operation cannot be neglected and must be included during the investigation of the COB structural response [18]. Since steady state analyses have been performed, the EM loads considered and used are relative to a specific instant of time, i.e. time step. During both NO and OP loading scenario, as prescribed by [16], the same EM loads have been considered. In particular, only the ferromagnetic loads contribution is considered, since the Lorentz's forces one is negligible. Instead, this assumption cannot be done for the UVDE loading scenario and the Lorentz's forces needs to be taken into account. So, as already done in [19], the EM loads related to two different time steps have been considered for the thermo-mechanical evaluation under the UVDE loading scenario: the time steps corresponding to the maximum of the radial forces and moment, t=11.52 s and t=11.585 s respectively. Thanks to a purposely developed computational procedure, the EM loads', calculated separately through a dedicated electro-magnetic analysis, have been applied onto the node mesh of the COB segment model. In particular, this procedure allows matching the cloud of points on which the EM forces are calculated to the structural analysis mesh. Since the former is much coarser than the latter, the developed procedure

is capable of assigning the EM forces calculated at the point (x, y, z) to the closest node of the structural analysis mesh. Since the EM model take into account the presence of breeder and DWTs, which are absent in the COB segment FEM model, the EM values in that regions have been allocated to the nearby Eurofer portion in order to conservatively consider their effects.

4.2. Results

Steady state analyses of the reference COB segment under different loading scenarios have been performed with the aim of evaluating its structural behaviour, as well as verifying that the safety criteria of the RCC-MRx for the structural material are fulfilled.

So, the Von Mises equivalent stress fields obtained for each different loading scenario are reported in Figure 11 and Figure 12, in which only the Eurofer structural material is displayed. The deformed vs. undeformed shapes are likewise depicted in Figure 13 and Figure 14, also with the displacement fields for each assessed scenario. In particular, the deformed shapes are showed with an isotropic amplification factor equal to 20. Looking at the displacement fields, in each operating scenario analysed, the maximum displacement occurs along the radial direction, as well as, looking the Von Mises stress fields, the equatorial region being the particularly stressed one. In Table 5 the maximum and minimum values of displacement along all directions for all the assessed scenarios are reported, where Ur, Ut and Up indicates the displacements along the radial, toroidal and poloidal direction respectively. The values obtained show the same trend and the largest displacement occurs in all the assessed scenarios along the radial direction, with the highest value raised in the OP loading scenario. Moreover, in the UVDE scenario, when the EM loads are considered at the time step of 11.585 s (maximum of radial moments), a larger displacement in toroidal direction than in the other scenarios can be highlighted.

Table 5. Maximum and minimum displacements values obtained

	NO	**OP**	**UVDE (t=11.52 s)**	**UVDE (t=11.585 s)**
Ur, max [mm]	40.3461	40.5314	37.9137	40.3827
Ur, min [mm]	-9.71531	-9.59273	-9.58886	-9.56706
Ut, max [mm]	5.46014	5.59649	6.19565	7.99158
Ut, min [mm]	-5.0945	-4.82734	-5.11112	-12.4684
Up, max [mm]	23.7326	23.5357	23.9653	23.9025
Up, min [mm]	-5.01018	-5.88849	-4.63463	-5.45198

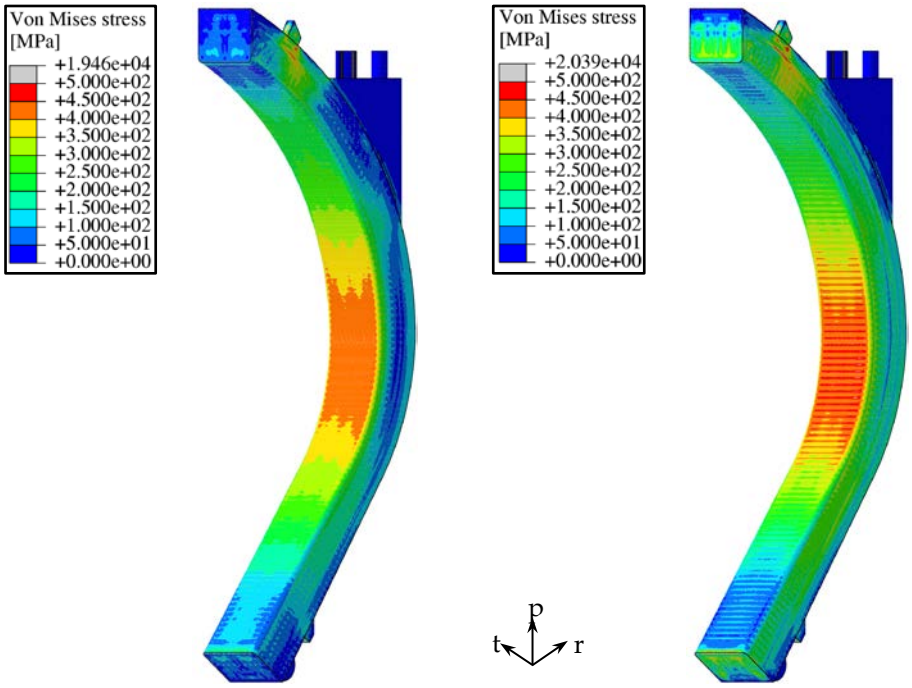

Figure 11. Von Mises stress field under NO and OP loading scenarios.

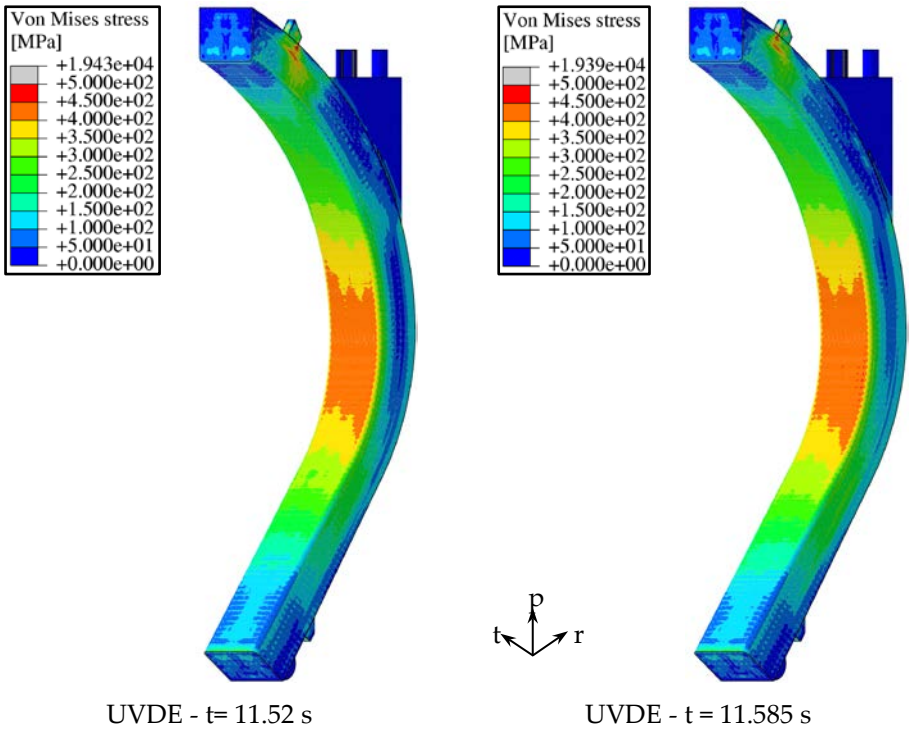

Figure 12. Von Mises stress field under UVDE (t=11.52 s and t=11.585 s) loading scenarios.

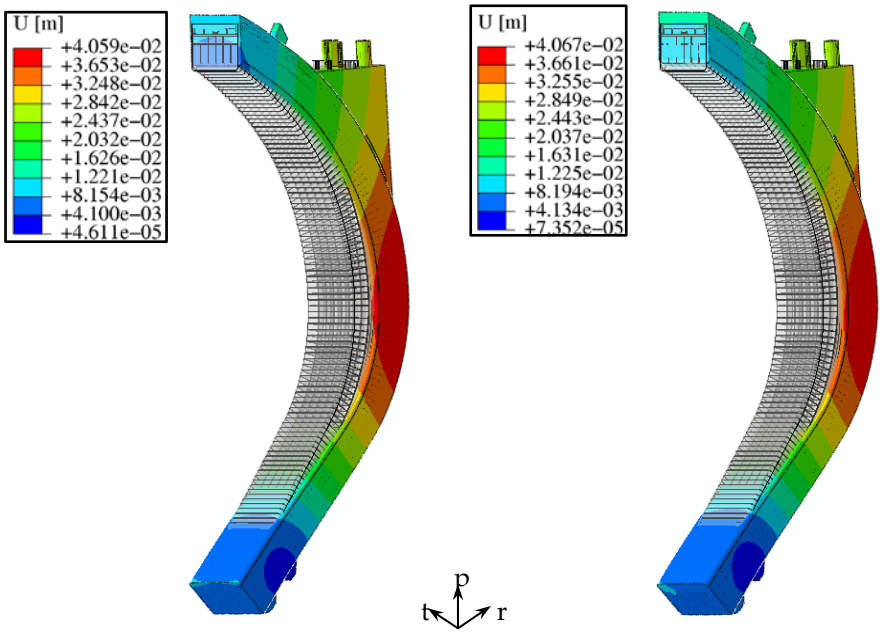

Figure 13. Deformed vs. Undeformed shapes under NO and OP loading scenarios.

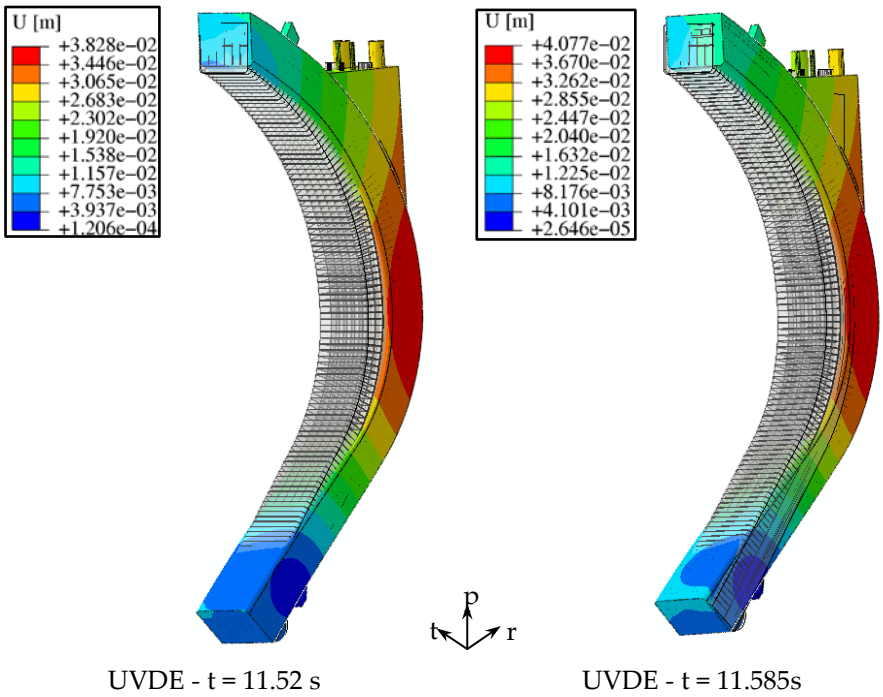

Figure 14. Deformed vs. Undeformed shapes under UVDE (t=11.52 s and t=11.585 s) loading scenarios.

In the end, a stress linearization procedure has been performed along some significant paths located within the most stressed regions of the structure and, then, the fulfilment of Level A, C and D criteria, namely for the NO, UVDE and OP loading scenario respectively, prescribed by the RCC-MRx design code along them has been checked. In particular, four criteria have been taken into account for the structural evaluation: Immediate Excessive Deformation (IED), Immediate Plastic Instability (IPI), Immediate Plastic Flow Localization (IPFL) and Immediate Fracture due to exhaustion of ductility

(IF). While the first two criteria only consider the primary stresses, the others also take into account secondary stresses occurring along the analysed path. For each criterion, the stress limit values have been calculated, for the service level (A, C or D) to which each loading scenario analysed relates, in accordance with the structural material and the average path temperature. Therefore, since the cooling channels located within the FW-SW region have not been modelled to reduce the computational burden, only the SPs grid has been considered from the mechanical point of view and some paths lying on the poloidal-radial and toroidal-radial SPs (Figure 15), at three different poloidal height, highlighted in red and blue in Figure 15, have been individuated.

The obtained results are reported in Table 6, Table 7, Table 8 and Table 9, also representing the average temperature values arising within each path. For each criterion, the ratio between the equivalent stress value and the corresponding stress limit is reported in the tables where the values greater than 1 are highlighted in red, indicating that the criterion is not fulfilled within the selected path. The evaluation of the results of the RCC-MRx criteria, indicates that the vertical SPs are particularly stressed, in particular the path named SPv2, in each poloidal height considered. In each considered loading scenario, these paths do not fulfil totally the criteria against the immediate plastic flow localization, namely the $(P_m+Q_m)/S_{em}$, unlike the path within the central poloidal-radial SP which, due to its lower average temperature, verifies this criterion in every operating scenario and at every segment height considered. Moreover, also the path SPh1, located in the central part of a horizontal SP in the upper region does not fulfil the IPFL criterion, taken into account the secondary stresses. Globally, average temperatures are higher in the regions in which the criterion against the Immediate Plastic Flow Localization does not verify, as reported in tables. Therefore, high temperatures, together with the action of the selected attachment system, could contribute to the failure of the RCC-MRx criteria verification.

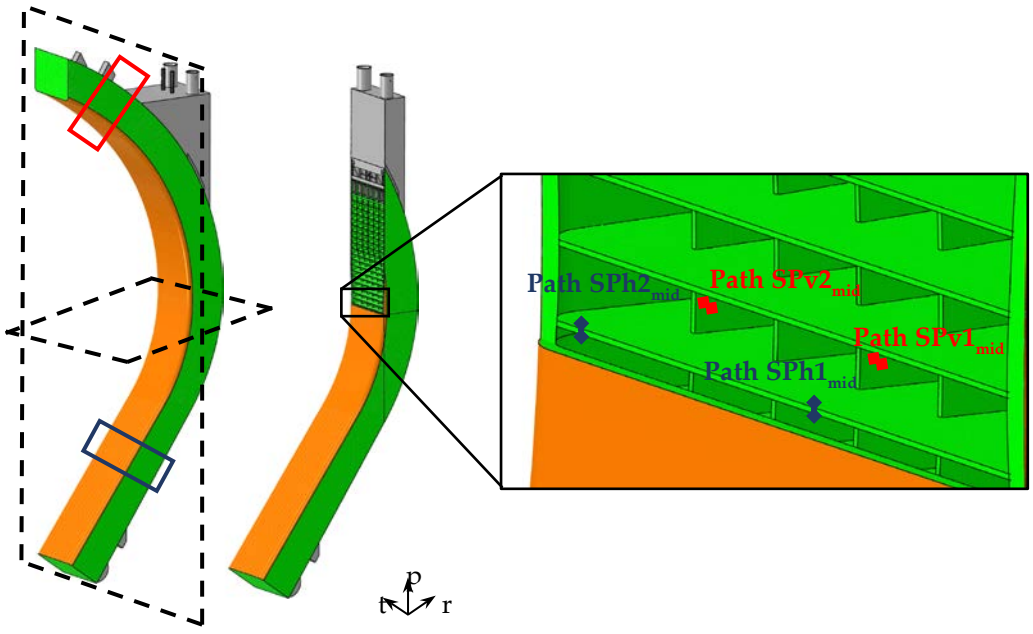

Figure 15. Paths within SPs grid in the equatorial region.

Table 6. Verification of RCC-MRx criteria under NO loading scenario.

Normal Operation					
	Tave [°C]	**Pm/Sm**	**(Pm+Pb)/(Keff·Sm)**	**(Pm+Qm)/Sem**	**(Pm+Pb+Q+F)/Set**
SPv1,mid	346.0	0.388	0.259	0.651	0.156
SPv2,mid	519.3	0.505	0.337	2.066	0.291
SPh1,mid	435.6	0.178	0.120	0.577	0.104
SPh2,mid	473.0	0.174	0.124	0.726	0.119
SPv1,top	325.4	0.452	0.302	0.328	0.078
SPv2,top	462.6	0.595	0.398	1.300	0.218
SPh1,top	400.6	0.084	0.067	1.029	0.216
SPh2,top	458.8	0.222	0.177	0.792	0.130
SPv1,bot	339.2	0.050	0.033	0.229	0.055
SPv2,bot	503.7	0.069	0.048	1.461	0.216
SPh1,bot	430.0	0.094	0.088	0.794	0.163
SPh2,bot	478.1	0.083	0.058	0.884	0.147

Table 7. Verification of RCC-MRx criteria under OP loading scenario.

Over-Pressurization					
	Tave [°C]	**Pm/Sm**	**(Pm+Pb)/(Keff·Sm)**	**(Pm+Qm)/Sem**	**(Pm+Pb+Q+F)/Set**
SPv1,mid	346.0	0.342	0.228	0.383	0.110
SPv2,mid	519.3	0.401	0.268	1.217	0.166
SPh1,mid	435.6	0.832	0.559	0.675	0.125
SPh2,mid	473.0	0.712	0.482	0.632	0.103
SPv1,top	325.4	0.214	0.142	0.312	0.089
SPv2,top	462.6	0.201	0.136	0.624	0.105
SPh1,top	400.6	0.725	0.486	0.957	0.213
SPh2,top	458.8	0.612	0.409	0.649	0.103
SPv1,bot	339.2	0.263	0.175	0.254	0.073
SPv2,bot	503.7	0.242	0.161	0.822	0.118
SPh1,bot	430.0	0.756	0.517	0.788	0.160
SPh2,bot	478.1	0.660	0.441	0.693	0.113

Table 8. Verification of RCC-MRx criteria under UVDE (t=11.52 s) loading scenario.

UVDE (t = 11.52 s)					
	Tave [°C]	**Pm/Sm**	**(Pm+Pb)/(Keff·Sm)**	**(Pm+Qm)/Sem**	**(Pm+Pb+Q+F)/Set**
SPv1,mid	346.0	0.273	0.182	0.553	0.1326
SPv2,mid	519.3	0.337	0.237	1.739	0.246
SPh1,mid	435.6	0.155	0.104	0.489	0.088
SPh2,mid	473.0	0.155	0.146	0.615	0.104
SPv1,top	325.4	0.291	0.195	0.263	0.063
SPv2,top	462.6	0.402	0.273	1.063	0.179
SPh1,top	400.6	0.076	0.060	0.865	0.182
SPh2,top	458.8	0.187	0.149	0.653	0.108
SPv1,bot	339.2	0.088	0.059	0.177	0.042
SPv2,bot	503.7	0.105	0.070	1.185	0.175
SPh1,bot	430.0	0.092	0.082	0.674	0.138
SPh2,bot	478.1	0.080	0.057	0.750	0.126

Table 9. Verification of RCC-MRx criteria under UVDE (t=11.585 s) loading scenario.

	UVDE (t = 11.585 s)				
	Tave [°C]	**Pm/Sm**	**(Pm+Pb)/(Keff·Sm)**	**(Pm+Qm)/Sem**	**(Pm+Pb+Q+F)/Set**
SPv1,mid	346.0	0.292	0.199	0.542	0.130
SPv2,mid	519.3	0.411	0.318	1.706	0.245
SPh1,mid	435.6	0.136	0.097	0.480	0.087
SPh2,mid	473.0	0.146	0.218	0.612	0.111
SPv1,top	325.4	0.322	0.217	0.281	0.068
SPv2,top	462.6	0.511	0.356	1.094	0.184
SPh1,top	400.6	0.085	0.064	0.865	0.182
SPh2,top	458.8	0.165	0.151	0.666	0.111
SPv1,bot	339.2	0.044	0.030	0.199	0.048
SPv2,bot	503.7	0.051	0.035	1.250	0.185
SPh1,bot	430.0	0.129	0.114	0.668	0.139
SPh2,bot	478.1	0.045	0.059	0.704	0.120

5. Conclusions

In the frame of the European DEMO BB research activities, a research campaign has been carried out with the aim of investigating the thermomechanical performances of the DEMO WCLL COB under NO, UVDE and OP steady state loading scenarios, ensuring the fulfilment of the thermal and structural design requirements, the latter represented by the RCC-MRx structural design criteria. Once optimized the cooling scheme from the thermal point of view, structural analyses have been performed.

All the assessed scenarios show a similar displacements field, with an evident radial displacement in the equatorial region suggesting a revision of the attachment system to limit the displacement in this direction of the structure.

Concerning the verification of the criteria of RCC-MRx design code, not all the criteria are verified in the paths taken into consideration and, especially, the criterion considering the secondary stresses, namely the Immediate Plastic Flow Localization, probably due to the resistance exerted by the SPs against the thermal expansion. Moreover, as the SB channels have not been modelled due to the modelling assumption, no path have been investigated within the highly stressed FW-SW region.

The study here reported allows concluding that the optimized WCLL COB segment geometric layout is promising also from the structural point of view, even though further analyses are necessary in order to study in detail the structural behaviour of the FW-SW region at different poloidal height of the COB segment, possibly adopting an update version of the attachment system.

Funding: This work has been carried out within the framework of the EUROfusion Consortium and has received funding from the Euratom research and training programme 2014 to 2018 and 2019 to 2020 under grant agreement No 633053.

Acknowledgments: The views and opinions expressed herein do not necessarily reflect those of the European Commission.

Author Contributions: Conceptualization, I. Catanzaro, G. Bongiovì and P. A. Di Maio; methodology, I. Catanzaro, G. Bongiovì and P. A. Di Maio; formal analysis, I. Catanzaro, G. Bongiovì and P. A. Di Maio; investigation, I. Catanzaro and G. Bongiovì; resources, I. Catanzaro, G. Bongiovì and P. A. Di Maio; data curation, I. Catanzaro and G. Bongiovì; writing—original draft preparation, I. Catanzaro and G. Bongiovì; writing—review and editing, I. Catanzaro, G. Bongiovì and P. A. Di Maio; visualization, I. Catanzaro and G. Bongiovì; supervision, P. A. Di Maio; project administration, P. A. Di Maio; funding acquisition, P. A. Di Maio. All authors have read and agreed to the published version of the manuscript.

Conflicts of Interest: The authors declare no conflict of interest.

Data Availability Statement: Data available on request from the authors.

References

1. F. Cismondi et al., Progress of the conceptual design of the European DEMO breeding blanket, tritium extraction and coolant purification systems, Fusion Engineering and Design, Volume 157, 2020, 111640, https://doi.org/10.1016/j.fusengdes.2020.111640.
2. G. Federici et al., An overview of the EU breeding blanket design strategy as an integral part of the DEMO design effort, Fusion Engineering and Design, Volume 141, 2019, pages 30-42, https://doi.org/10.1016/j.fusengdes.2019.01.141.
3. P. Arena et al., The DEMO Water-Cooled Lead-Lithium Breeding Blanket: design status at the end of the Pre-Conceptual Design Phase, Applied Sciences, 11 (24), 11592, 2021, https://doi.org/10.3390/app112411592.
4. S. D'Amico et al., Preliminary thermal-hydraulic analysis of the EU-DEMO Helium-Cooled Pebble Bed fusion reactor by using the RELAP5-3D system code, Fusion Engineering and Design, Volume 162, 2021, https://doi.org/10.1016/j.fusengdes.2020.112111.
5. I. Catanzaro, Development and application of an alternative modelling approach for the thermo-mechanical analysis of a DEMO Water-Cooled Lithium Lead breeding blanket segment, 2021, under review.
6. RCC-MRx, Design and Construction Rules for Mechanical Components of Nuclear Installations, AFCEN, 2013.
7. Abaqus Analysis User's Guide: Online Documentation. Version 6.14-2, Providence, RI, Simulia, Dassault System.
8. F. Maviglia, Z. Vizvary, M.L. Richiusa, J. Gerardin, M. Firdaouss, DEMO PFC Surface Heat Load Specifications (2020), EFDA IDM Ref. EFDA_D_2P985Q.
9. E. Gaganidze, Material Properties Handbook – EUROFER97 (2020), EFDA IDM Ref. EFDA_D_2NZHBS
10. D. Martelli, A. Venturini, M. Utili, Literature review of lead-lithium thermophysical properties, Fusion Engineering and Design, (138) 2018, 183-195, DOI: 10.1016/j.fusengdes.2018.11.028
11. E. Gaganidze, F. Schoofs, Material Properties Handbook – Tungsten (2020), EFDA IDM Ref. EFDA_D_2P3SPL
12. F. Maviglia, DEMO PFC Surface Heat Load Specification (2020), EFDA IDM Ref. EFDA_D_2P985Q
13. T. Berry, T. Eade, Activation analysis and evaluation of inventories, decay heat, for important components – Activity 2019 – CCFE contribution (Calculation of decay heat in PbLi for entire WCLL reactor), EFDA IDM Ref. EFDA_D_2NQL5P
14. F. P. Incropera et al, Principles of heat and mass transfer, 7th edition
15. P.A. Di Maio et al., On the numerical assessment of the thermo-mechanical behaviour of the DEMO Water Cooled Lithium Lead equatorial outboard blanket module, Fusion Engineering and Design, vol. 124, 725-729, 2017, DOI: 10.1016/j.fusengdes.2017.05.051.
16. G. A. Spagnuolo et al., Development of load specifications for the design of the breeding blanket system, Fusion Engineering and Design, 157, 111657, 2020, DOI: 10.1016/j.fusengdes.2020.111657
17. C. Bachmann, et al., IDD – Blanket Mechanical Supports (2019) EFDA IDM Ref. EFDA_D_2NHC86
18. I.A. Maione et al., Analysis of EM loads on DEMO WCLL Breeding Blanket during VDE-up, Fusion Engineering and Design, 136 (2018), 1523-1528, DOI: 10.1016/j.fusengdes.2018.12.017
19. I. Catanzaro et al., Structural assessment of the EU DEMO WCLL Central Outboard Blanket segment under normal and off-normal operating conditions, Fusion Engineering and Design, 167, 112350, 2021, DOI: 10.1016/j.fusengdes.2021.112350